THE JOURNAL OF BIOLOGICAL CHEMISTRY Vol. 279, No. 5, Issue of January 30, pp. 3142–3150, 2004
Printed in U.S.A.

Identification and Characterization of TRP14, a Thioredoxin-related Protein of 14 kDa

NEW INSIGHTS INTO THE SPECIFICITY OF THIOREDOXIN FUNCTION*

Received for publication, July 21, 2003, and in revised form, October 15, 2003
Published, JBC Papers in Press, November 7, 2003, DOI 10.1074/jbc.M307932200

Woojin Jeong‡§¶, Hae Won Yoon‡¶‖, Seung-Rock Lee‡, and Sue Goo Rhee‡ ‡‡**

From the ‡Laboratory of Cell Signaling, NHLBI, National Institutes of Health, Bethesda, Maryland 20892 and the §Center for Cell Signaling Research, Ewha Women's University, Seoul 120-750, Korea

We have identified and characterized a 14-kDa human thioredoxin (Trx)-related protein designated TRP14. This cytosolic protein was expressed in all tissues and cell types examined, generally in smaller amounts than Trx1. Although TRP14 contains five cysteines, only the two Cys residues in its WCPDC motif were exposed and redox sensitive. Unlike Trx1, which was an equally good substrate for both Trx reductase 1 (TrxR1) and TrxR2, oxidized TRP14 was reduced by TrxR1 but not by TrxR2. Biochemical characterization of TRP14 suggested that, like Trx1, TRP14 is a disulfide reductase; its active site cysteine is sufficiently nucleophilic with the pK_a value of 6.1; and its redox potential (−257 mV) is similar to those of other cellular thiol reductants. However, although TRP14 reduced small disulfide-containing peptides, it did not reduce the disulfides of known Trx1 substrates, ribonucleotide reductase, peroxiredoxin, and methionine sulfoxide reductase. These results suggest that TRP14 and Trx1 might act on distinct substrate proteins.

The redox state of cysteine residues, on which the structure and function of many proteins depend, is maintained by intracellular redox-regulatory molecules such as thioredoxin (Trx).[1] Central to the redox-regulatory function of Trx is the ability of the reduced form of the molecule to recognize and reduce proteins containing a disulfide (1, 2). The reducing equivalents are provided by two redox-active cysteines (Cys^{32} and Cys^{35} in mammalian Trx1) that are located within a WCGPC motif (also called C*XX*C motif) that is conserved among Trx molecules from all species (1–4). Because the pK_a for the N-terminal Cys of the WCGPC motif is substantially lower than the usual value of 8.5 for cysteine residues (5), this Cys exists at neutral pH as a thiolate anion ($Cys\text{-}S^-$), which is more reactive than protonated cysteine. After Trx1 (consisting of 105 amino acids) binds to the oxidized substrate, the thiolate of Cys^{32} of Trx1 forms a transient mixed disulfide with the substrate that is subsequently attacked by Cys^{35} to generate oxidized Trx1 and reduced substrate.

Substrates for the disulfide reductase activity of Trx1 include ribonucleotide reductase (RNR); peroxiredoxin (Prx); methionine sulfoxide reductase (MSR); PTEN (a 3-phosphatase for phosphoinositides) (6–10); several transcription factors, including nuclear factor-κB (NF-κB) (4, 11–13); redox factor-1 (Ref-1), and an enhancer of the DNA binding activity of activator protein-1 (AP-1) (14). RNR, Prx, and MSR generate a disulfide-containing intermediate during catalysis, the reduction of which by Trx1 is essential for catalytic function. PTEN and certain transcription factors contain H_2O_2-sensitive cysteines, the oxidation of which inactivates their enzymatic and DNA binding activities, respectively.

Trx1 also regulates protein function by binding to target proteins without affecting their redox state. For example, Trx1 in its reduced form binds to and thereby inhibits the activity of apoptosis signal-regulating kinase 1 (ASK1) (15–17), an upstream activator of c-Jun N-terminal kinase (JNK) and p38 mitogen-activated protein kinase (MAPK) signaling pathways. Oxidation of the Cys residues of the WCGPC motif of Trx1 induces dissociation of the Trx1-ASK1 complex, releasing the inhibitory effect of Trx1. Trx1 also binds in a redox-sensitive manner to vitamin D_3 up-regulated protein 1 (VDUP1) (18). Because thiolate anions are more sensitive to oxidation than are protonated thiols, the two Cys residues of the WCGPC motif of Trx1 readily form a disulfide in the presence of oxidants. Thus, Trx1 is able to serve as a redox sensor and transducer that imparts information on cellular redox status to proteins that do not possess their own redox-sensitive residues.

The various substrates for the disulfide reductase activity of Trx1 and the targets for the redox-transducer role of this protein share no apparent structural similarity. Nevertheless, Trx1 interacts with these proteins with a relatively high affinity, as indicated by the micromolar range of K_m values for RNR and Prx (19–21), the co-immunoprecipitation of Trx1 with ASK1 or PTEN (10, 15, 22), and detection of the association of Trx1 with Ref-1 or ASK1 by yeast two-hybrid system (14, 15). The interaction appears to be specific, given that oxidized Prx and PTEN are substrates for Trx1 but not for glutaredoxin (Grx), another redox mediator that contains the C*XX*C motif (10, 23, 24); that oxidized NF-κB is reduced by Trx1 but not by glutathione (GSH) and GSH reductase (11); and that Trx1 and Grx inhibit ASK1 activity by binding to the N- and C-terminal

* This work was supported in part by the Korean Science and Engineering Foundation Center of Excellence grant to the Center for Cell signaling Research at Ewha Women's University (to W. J.). The costs of publication of this article were defrayed in part by the payment of page charges. This article must therefore be hereby marked "*advertisement*" in accordance with 18 U.S.C. Section 1734 solely to indicate this fact.

¶ Both authors contributed equally to this work.
‖ Present address: Division of Applied Life Science (BK21 program), Gyeongsang National University, Jinju, Gyeongnam 660-701, Korea.
** Present address: Center for Cell Signaling Research, Ewha Women's University, Seoul 120-750, Korea.
‡‡ To whom correspondence should be addressed: Bldg. 50, Room 3523, South Drive, MSC 8015, Bethesda, MD 20892. Tel.: 301-496-9646; Fax: 301-480-0357; E-mail: sgrhee@nih.gov.

[1] The abbreviations used are: Trx, thioredoxin; RNR, ribonucleotide reductase; Prx, peroxiredoxin; MSR, methionine sulfoxide reductase; PTEN, a 3-phosphatase for phosphoinositides; ASK1, apoptosis signal-regulating kinase 1; Grx, glutaredoxin; TRP14, 14-kDa thioredoxin-related protein; TrxR1, Trx reductase 1; DTNB, 5,5′-dithiobis(2-nitrobenzoic acid); MES, 4-morpholineethanesulfonic acid.

regions of the kinase, respectively (22). Nuclear magnetic resonance analysis of the structure of Trx1 complexed with several target proteins (or peptides) has revealed that the active site surface relies on different combinations of amino acid residues to provide the binding sites required for the recognition of such proteins (25). Nevertheless, given the large number of proteins that undergo reversible disulfide formation in response to changes in cellular redox state (26), it is likely that additional Trx-like proteins support specific reduction reactions.

We have now identified a 14-kDa cytosolic protein, designated Trx-related protein 14 (TRP14), which contains a WCPDC motif. To demonstrate that TRP14 has the potential to serve as a disulfide reductase like Trx, we evaluated its biochemical properties including identification of the redox-sensitive cysteines and determination of its redox potential and pK_a. Comparison of these properties with those of Trx1 suggests that the disulfide reductase activities of the two proteins are similar. Indeed, TRP14 and Trx1 reduced small disulfide-containing peptides at similar rates. However, TRP14 exhibited negligible disulfide reductase activity with three known Trx1 substrates RNR, Prx, and MSR. These results suggest the specificity of disulfide reductase reaction.

EXPERIMENTAL PROCEDURES

Materials—Rat Trx reductase 1 (TrxR1) and TrxR2 were purified from liver and specific antisera to these proteins were prepared as described (27). Recombinant rat Trx1 and human PrxI were prepared as described (8). RNR and MSR were kindly provided by B. Cooperman (Department of Chemistry, University of Pennsylvania) and J. Moskovitz (NHLBI, National Institutes of Health), respectively. Rabbit antiserum to human TRP14 was produced by injection of the purified protein according to standard procedures. Insulin, NADPH, and $NADP^+$ were purchased from Calbiochem. Oxytocin, vasopressin, and iodoacetamide were from Sigma, and iodo[1-^{14}C]acetamide was from Amersham Biosciences.

Cloning and Mutagenesis of Human TRP14—The DNA sequence encoding human TRP14 was amplified by PCR from a HeLa cell cDNA library (Clontech) with a forward primer (5′-GTCGTGCATATGGCCC-GCTATGAGGAGGTGAGC-3′) containing both an NdeI site (underlined) and the initiation codon (bold) and with a reverse primer (5′-CGCGGATCCTTAATCTTCAGAGAACAACATTTCC-3′) containing both a BamHI site (underlined) and the stop codon (bold). The PCR product was purified, digested with NdeI and BamHI, and cloned into the corresponding sites of the pET-11a vector for expression in *Escherichia coli* (*E. coli*). Two TRP14 mutant proteins, C43S and C46S, in which Cys^{43} and Cys^{46} are individually replaced by serine, were generated by standard PCR-mediated site-directed mutagenesis with complementary primers containing a 1-bp mismatch that converted the codon for cysteine to one for serine. The PCR products were digested with NdeI and BamHI and then ligated into the corresponding sites of pET-11a.

Purification of Recombinant Human TRP14—E. coli BL21(DE3) transformed with pET-11a encoding wild-type or mutant TRP14 proteins was cultured at 37 °C, in LB medium supplemented with ampicillin (100 μg/ml), until the optical density of the culture at 600 nm reached 0.5 to 0.6. Isopropyl-β-D-thiogalactopyranoside was then added to the culture at a final concentration of 0.4 mM, and after incubation for an additional 3 h, the cells were harvested by centrifugation and stored at −70 °C until use. The frozen cells were suspended in 20 mM HEPES-NaOH (pH 7.0) containing 1 mM EDTA and 1 mM 4-(2-aminoethyl)benzene-sulfonyl fluoride, and disrupted by sonication. After removal of nucleic acid with streptomycin sulfate, proteins were precipitated by slowly adding solid ammonium sulfate to 80% saturation and dissolved in 20 mM HEPES-NaOH (pH 7.0) containing 1 mM EDTA and 1 M ammonium sulfate. After clarification, the soluble fraction was applied at a flow rate of 5 ml/min to a TSK Phenyl-5PW column (21.5 by 150 mm) that had been equilibrated with 20 mM HEPES-NaOH (pH 7.0) containing 1 mM EDTA and 1 M ammonium sulfate. The flow-through fraction was collected, concentrated by ultrafiltration (Amicon YM10 device), and then dialyzed against 20 mM Tris-HCl (pH 7.4) containing 1 mM EDTA. The dialyzed sample was applied to a Mono Q HR 10/10 column (Amersham Biosciences) that had been equilibrated with 20 mM Tris-HCl (pH 7.4) containing 1 mM EDTA. Proteins were eluted from the column with a linear gradient of NaCl from 0 to 0.3 M over 60 min at a flow rate of 2 ml/min. The fractions corresponding to the peak of TRP14 were pooled and dialyzed against 10 mM HEPES-NaOH (pH 7.0).

Determination of Protein Concentration—The concentrations of recombinant human TRP14 as well as of rat Trx1, TrxR1, and TrxR2 were determined spectroscopically with A_{280} values for 0.1% solutions of 1.293, 0.738, 0.937, and 1.077, respectively, calculated on the basis of amino acid composition. The concentrations of other proteins were determined by the Bradford method with bovine serum albumin as a standard.

RESULTS

cDNA Cloning, Genomic Organization, and Sequence Analysis of the Human TRP14 Gene—We previously developed a procedure for the detection of proteins that contain a ROS-sensitive cysteine residue with a low pK_a (26). This procedure detected a rat brain protein that contains a reactive Cys conforming to the WC*XX*C motif (the C*XX*C sequence is preceded by W in Trx proteins and by Y in Grx proteins); the sequence of the alkylated peptide obtained after digestion of the protein with the endoproteinase Lys-C was determined as SWCPD-CVEAEPIIREGLK (data not shown). A homology search of the GenBank™ data base with this peptide sequence using BLAST program yielded the human cDNA clones ZC48G12 (GenBank™ accession number, AF086210) and MGC14353 (GenBank™ accession number, BC006405). The DNA sequence of MGC14353 consists of an open reading frame of 372 bp, a 5′-untranslated region of 68 bp including an in-frame stop codon (TAG), and a 3′-untranslated region containing two putative polyadenylation signals (AATAAA) (Fig. 1*A*). The ZC48G12 clone contains a shorter 3′-untranslated region and may have originated from an mRNA whose transcription was terminated by the first polyadenylation signal. The predicted open reading frame encodes a protein of 123 amino acids with a calculated molecular mass of 14 kDa and an isoelectric point of 5.4. This protein shares 20% sequence identity and 37% similarity with human Trx1 (Fig. 1*B*) and was therefore designated Trx-related protein 14 (TRP14). We cloned the TRP14 cDNA from a HeLa cell cDNA library.

A BLAT search of the working draft of the human genome sequence revealed that the gene for TRP14 is located at chromosome 17p13.1 and comprises four exons as well as three introns that conform to the GT/AG rule. The predicted protein does not contain a known signal peptide for targeting to a specific subcellular compartment, and subcellular fractionation of HeLa cell homogenates into organellar, plasma membrane, and cytosolic fractions revealed TRP14 to be enriched in the cytosolic fraction (data not shown). A BLAST homology search of the GenBank™ data base yielded several TRP14 homologs in a wide range of species from bacteria to mammals (Fig. 1*C*). Sequence alignment of these homologous proteins revealed that the WCPDC motif was fully conserved, indicating the potential importance of this motif in TRP14 function.

Cellular and Tissue Distribution of TRP14—Total soluble fractions prepared from rat tissues and cultured human cells were subjected to immunoblot analysis with antibodies specific for TRP14 or for Trx1. The specificity of the antibodies is shown in Fig. 2*A*. TRP14 was detected in all tissues examined, being most abundant in liver, kidney, pancreas, and uterus (Fig. 2*B*). Although TRP14 appeared to be present in smaller amounts than Trx1 in most of the cell lines examined, like Trx1 it seemed to be ubiquitous (Fig. 2*C*). Comparison of immunoblot intensities with those of protein standards yielded estimates of 0.3 and 1.8 μg/mg of cell lysates for the amounts of TRP14 and Trx1, respectively, in HeLa cells (Fig. 2*D*).

The CXXC Motif of TRP14 Is a Redox Active Site—TRP14 contains three cysteine residues (Cys^{64}, Cys^{69}, Cys^{110}) in addition to the conserved Cys^{43} and Cys^{46}. To examine the oxida-

A

```
   1 ggcacgaggggacccaaccgcggcgaccggacgtgcactcctccagtagcggctgcacg
  61 tcgtgccaatggcccgctatgaggaggtgagcgtgtccggcttcgaggagttccaccggg
           M  A  R  Y  E  E  V  S  V  S  G  F  E  E  F  H  R   17
 121 ccgtggaacagcacaatggcaagaccatttttcgcctactttacgggttctaaggacgccg
     A  V  E  Q  H  N  G  K  T  I  F  A  Y  F  T  G  S  K  D  A   37
 181 gggggaaaagctggtgccccgactgcgtgcaggctgaaccagtcgtacgagaggggctga
     G  G  K  S  W  C  P  D  C  V  Q  A  E  P  V  V  R  E  G  L   57
 241 agcacattagtgaaggatgtgtgttcatctactgccaagtaggagaaaagccttattgga
     K  H  I  S  E  G  C  V  F  I  Y  C  Q  V  G  E  K  P  Y  W   77
 301 aagatccaaataatgacttcagaaaaaacttgaaagtaacagcagtgcctacactactta
     K  D  P  N  N  D  F  R  K  N  L  K  V  T  A  V  P  T  L  L   97
 361 agtatggaacacctcaaaaactggtagaatctgagtgtcttcaggccaacctggtggaaa
     K  Y  G  T  P  Q  K  L  V  E  S  E  C  L  Q  A  N  L  V  E  117
 421 tgttgttctctgaagattaagatttaggatggcaatcatgtcttgatgtcctgatttgt
     M  L  F  S  E  D  *                                        123
 481 tctagtatcaataaactgtatacttgctttgaattcatgttagcaataaatgatgttaaa
 541 aaaaaaaaaaaaaaaaaaaaaaaaaaaaaaaaaaaaaaaa
```

B

```
TRP14   1  MARYEEVSVSGFEEFHRAVEQHNGKTIFAYFTGSKDAGGKSWCPDCVQAEPVVREGLKHISEGCVFIYCQ  70
Trx1    1  MVKQIESKTA----FQEALDAAGDKLVVVDFS-------ATWCGPCKMIKPFFHS-LSEKYSNVIFLEVD  58

TRP14  71  VGEKPYWKDPNNDFRKNLKVTAVPTLLKYGTFQKIVESECLQANIVEMLFSED-  123
Trx1   59  VDD-------CQDVASECEVKCMPTFQFFKKGQKVGEFSGANKEKLEATINELV  105
```

C

```
Human          1  MARYEEVSVSGFEEFHRAVEQHN-------GKTIFAYFTGSKDAG-GKSWCPDCVQAEPVVREGLK---HIS-EGCVFIY  68
Bovine         1  MASYEEVSVSGYEEFMQVVEQHS-------DKTIFAYFSGSKDAE-GKSWCPDCVQAEPVVREGLK---HVG-EGCVFIY  68
Rat            1  MATFEEVSVLGFEEFDKAVKEHQ-------GKTIFAYFSGSKDTE-GKSWCPDCVEAEPIIREGLK---HVT-EDCVFIY  68
Mouse          1  MATFEEVSVLGFEEFDKAVKEHE-------GKTIFAYFSGSKDTE-GKSWCPDCVEAEPVIREGLK---HVT-EDCVFIY  68
Silkworm       1  --MVINLDLKGFEEFSKYTRAIDS-----RGPPVFFYFSGSKLPD-GNSWCPDCVEAEPVVRHYLS---ELD-KSIIFVY  68
Fruitfly       1  --MPEYVPARGFKEMENLIKLYEN-----QRSPIYIYFYGEKDKD-GRSWCPDCVAAEETIMSAFRN--HAP-ADCMILV  69
Nematode       1  ----NTTLLRDTKHFRETLKSIG------KGKRVVALFTGSKILTTGESWCPDCVVAEPVVEEVLKDAAVAG-LDVHFVT  69
Soybean        1  --MPLKVLEATVSSFDVVFEKFRS--EAPQNKANLILFLADNDPATSLSWCPDCVRAEPVIYKKLEASPD----DIALLR  72
Tomato         1  --MRPKVLDATITTFDGVFEKFKA--ESPKNKANFILFLADIDPSTNLSWCPDCVRAEPALYKKLEASYD----DIALLR  72
Thale-cress    1  --MTLKKVDANPSTLESSLQELKSD-ETSRSKINFILFLADNDPTTGQSWCPDCVRAEPVIYKTLEEFPE----EVKLIR  73
Rice           1  --MTVEKVDATVADFFDAHFDKLFAAGDDAEGKVKLLLFLADRDASSNQTWCPDCNVAEPVIYDRVEAAAKGKEKDVVLLR  78
Chlamydomonas  1  --MAASVIKANVSTWSSKLAELEQ-----APSPHYIVFTGYDAAG--AMWCPDCVRAVPAVLRAAAAAPG------TLLE  65
Yeast          1  -------MSAFVTKAEEMIKSHP-------------YFQLS------ASWCPDCVYANSIWNK-LN-------VQDKVFV  46
Helicobacter   1  -----MSEMINGKNYAEKIAHQA-----------VVVNVG-------ASWCPDCRKIEPIMEN--------------LAK  43

Human         69  CQVGEKPYWK-DPNNDFRKN--LKVTAVPTLLKYG----TPQKLV--ESECLQANLVEMLFSED----------  123
Bovine        69  CQVGEKPYWK-DPNNDFRKN--LKLTAVPTLLKYG----TPQKLV--ESECLQANLVEMLFSED----------  123
Rat           69  CQVGDKPYWK-DPNNDFRQK--LKITAVPTLLKYG----TPQKLV--ESECRQSNLVEMIFSED----------  123
Mouse         69  CQVGDKPYWK-DPNNDFRQK--LKITAVPTLLKYG----TPQKLV--ESECCQSSLVEMIFSED----------  123
Silkworm      69  VDVGDREYWK-DKECPERTDSRSKLMVIPTLIKWK----GVQRLE--GSQCSNRELLQMLFEEDD---------  126
Fruitfly      70  VDVGSRESWI-GKDNMFRKPP-YSVEGIPTLIRWK----GVERLD--GDQLLKSSLLELFFEETDPKKSNFVAQ  135
Nematode      70  VFVGNREVWR-DPAVGFRTDPTLKLICIPTLLEVGN---KAKRLL--ERQIANKHLVKDFFTEED---------  128
Soybean       73  AYVGDRPTWR-NPQHPWRVDPRFKLTGVPTLIRWENN-TVKGRLE--DHEAHLENKIEALVADK----------  132
Tomato        73  AYVGDRPTWR-TPQHPWRVDGRFNLKGVPTLIRWEND-AIKGRLE--DHEAHLDHKIGSLLNEA----------  132
Thale-cress   74  AYAGDRPTWR-TPAHPWRVDSRFKLIGVPTLVRWDGD-SVKGRLE--DHQAHLPHLILPLLAPST---------  134
Rice          79  AYVGDKPTWR-DPAHPWRADPRFRLTGVPTLIRWENG-AEAARLG--DDEAHLADKVDAVVNAAN---------  139
Chlamydomonas 66  VDVGQRTDWRGNATHPERTAPALKLTGIPTLLQWGGG-AAVKRLGPELEACGSPAEVEALLAKSGFFQ------  132
Yeast         47  FDIGSLPRNE-QEKWRIAFQKVVGSRNLPTIVVNGKFWGTESQLHRFEAKGTLEEELTKIGLLP----------  109
Helicobacter  44  TYKGKVEFFKVSFDESQDLKESLGTRKIPTLIFYKNAKEVGERLVEPSSQKPIEDALKALL------------  104
```

FIG. 1. **Nucleotide and amino acid sequences of human TRP14 and homologous proteins.** *A*, nucleotide sequence and deduced amino acid sequence of human TRP14 cDNA. The nucleotide sequence is that of human clone MGC14353 (GenBank™ accession number BC006405). Nucleotide and amino acid residue numbers are shown on the *left* and *right*, respectively. The initiation (ATG) and termination (TAA) codons are indicated in *bold*. The putative active site sequence C*XXC* is *boxed*. Polyadenylation signals (AATAAA) and an upstream in-frame stop codon (TAG) are *underlined*. *B*, alignment of the amino acid sequences of human TRP14 and Trx1. *Black* and *gray boxes* indicate identical and similar residues, respectively. *C*, sequence alignment of TRP14 homologs. The deduced amino acid sequences of human (GenBank™ accession number, AF086210), *Bos taurus* (bovine, AW346357), *Rattus norvegicus* (rat, AW917424), *Mus musculus* (mouse, NM_026559), *Bombyx mori* (silkworm, AU003992), *Drosophila melanogaster* (fruit fly, CAB58075), *Caenorhabditis elegans* (nematode, AV193251), *Glycine max* (soybean, AW734061), *Lycopersicon esculentum* (tomato, AW223476), *Arabidopsis thaliana* (thale-cress, BAB09186), *Oryza sativa* (rice, BE040654), *Chlamydomonas reinhardtii* (BE056551), *Saccharomyces cerevisiae* (yeast, NP013468), and *Helicobacter pylori* (B64702) proteins were aligned with the use of the CLUSTAL X (1.8) multiple sequence alignment program. *Black* and *gray boxes* indicate identity and similarity, respectively.

tion status of these Cys residues, we quantified the thiol content of reduced and oxidized forms of TRP14 by spectrophotometric titration with 5,5′-dithiobis(2-nitrobenzoic acid) (DTNB) under nondenaturing or denaturing (6 M guanidinium chloride) conditions. Only two of the five cysteine residues in the reduced native enzyme were available for oxidation by DTNB or H_2O_2; the remaining three Cys residues remained unmodified in the native protein (Table I).

To investigate which cysteine residues are redox sensitive, we analyzed peptides derived from oxidized or reduced TRP14. The free SH groups of TRP14 were masked with iodoacetamide under denaturing conditions, the protein was digested with Lys-C, and the resulting peptides were resolved by reversed-phase high-performance liquid chromatography (HPLC) (Fig. 3). Comparison of the elution profiles of reduced and oxidized TRP14 indicated that peak *b* corresponds to a peptide with a

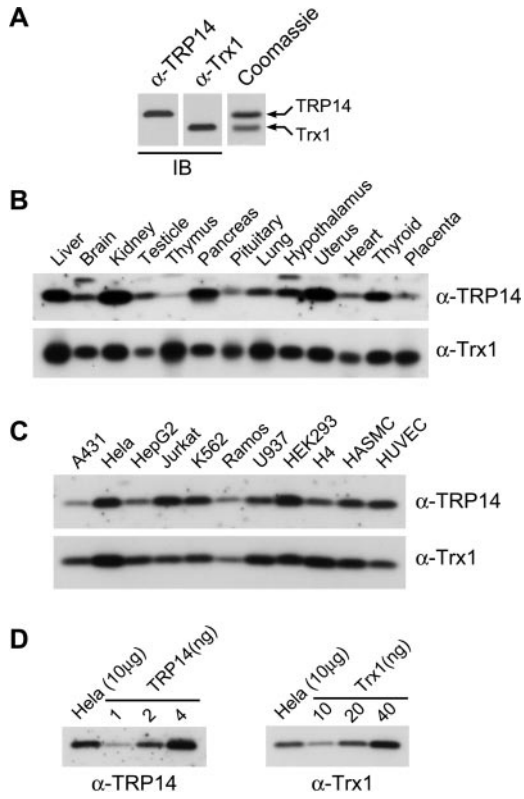

FIG. 2. **Distribution of TRP14 and Trx1 in rat tissues and human cell lines.** *A*, the specificity of rabbit antibodies to TRP14 and Trx1. A mixture of recombinant TRP14 and Trx1 was separated on a 14% SDS gel and detected by Western blot (*left panel*) or by Coomassie Brilliant Blue staining (*right panel*). *B*, tissue homogenates (20 and 2 μg of protein, respectively) were subjected to immunoblot analysis with rabbit antibodies to human TRP14 (α-TRP14) and to rat Trx1. *C*, cell lysates (10 μg) were subjected to immunoblot analysis with rabbit anti-human TRP14 and goat anti-human Trx1. HASMC, human aortic smooth muscle cells; HUVEC, human umbilical vein endothelial cells. *D*, relative abundance of TRP14 and Trx1 in HeLa cells. Cell lysates (10 μg) and the indicated amounts of purified recombinant human TRP14 or human Trx1 were subjected to immunoblot analysis with rabbit anti-human TRP14 and goat anti-human Trx1, as indicated.

disulfide linkage and that peak *a* corresponds to the reduced form of this peptide. Indeed, after reduction with DTT and modification with iodoacetamide, the purified peptide *b* eluted at a retention time identical to that of peptide *a*. Amino acid sequencing of peptides *a* and *b* revealed identical sequences of SWCPDCVQAEPVVREGLK. These results indicated that the conserved Cys residues (Cys^{43} and Cys^{46}) of TRP14 are oxidized by H_2O_2 and form an intramolecular disulfide bond that is sensitive to reduction by DTT.

Reduction of oxidized *E. coli* Trx was previously shown to increase tryptophan fluorescence by 2.5-fold (28–30). TRP14, which contains Trp^{77} and Trp^{42}, also produced a 2.6-fold increase in tryptophan fluorescence when reduced (Fig. 4), suggesting changes in the microenvironment around the two tryptophan residues.

TRP14 Is a Substrate for TrxR1 but Not TrxR2—Trx function requires a reversible change in the redox status of the C*XX*C motif. Reduction of oxidized Trx molecules is catalyzed by the NADPH-dependent enzyme Trx reductase (TrxR) (31, 32). Mammalian cells contain two isoforms of both Trx and TrxR: Trx1 and TrxR1 are localized predominantly to the cytosol, whereas Trx2 and TrxR2 are synthesized in the cytosol with a mitochondrial targeting sequence that results in their translocation into mitochondria (27, 33). The amino acid sequences of TrxR1 and TrxR2 are 54% identical (27). Although the overall amino acid sequence identity of Trx1 and Trx2 is only 35%, the active site sequence (WCGPCK) is conserved and both proteins are equally good substrates for TrxR1 or TrxR2 in the NADPH-dependent reduction reaction (27).

TABLE I
Determination of the thiol content of TRP14

Purified recombinant TRP14 was oxidized by incubation with a stoichiometric amount of H_2O_2. The reduced protein was prepared by incubation with a 10-fold molar excess of DTT and then isolated with a Sephadex G-25 (PD10) column. The thiol content of TRP14 was then determined by spectrophotometric titration with DTNB on the basis of extinction coefficients at 412 nm of 14,150 and 13,700 M^{-1} cm^{-1} for TNB^2 when the titration was performed under the native condition or in the presence of 6 M guanidinium chloride, respectively (51).

	Native	Denatured
Oxidized	0.12	3.09
Reduced	1.93	4.95

We examined whether oxidized TRP14 is reduced by TrxR1 in the presence of NADPH by monitoring NADPH oxidation at 340 nm. The reduction of oxidized TRP14 by TrxR1 occurred slightly faster than did that of oxidized Trx1 (Fig. 5*A*). The acceptor of the electrons from NADPH in TRP14 was shown to be the disulfide formed between Cys^{43} and Cys^{46} by the observation that two mutant proteins (C43S and C46S) in which these residues were individually replaced by serine did not support TrxR1-dependent NADPH oxidation (Fig. 5*B*). Performance of the NADPH oxidation reaction in the presence of various concentrations of TRP14 or Trx1 (data not shown) allowed determination of kinetic parameters by Michaelis-Menten analysis (Table II). The K_m and k_{cat} values were similar for the reduction of TRP14 and Trx1 by TrxR1, but the catalytic efficiency (k_{cat}/K_m) for the TRP14 reaction was slightly higher than that for the Trx1 reaction. In contrast, the reduction of TRP14 by TrxR2 was negligible compared with that of Trx1 (Fig. 5*C*). The reduction of TRP14 by GSH or glutathione reductase (GR) in the presence of NADPH was also negligible (data not shown).

TRP14 versus Trx1 as a Disulfide Reductase—The pK_a values of Cys residues in the C*XX*C motif are important determinants of reductase activity, given that initial nucleophilic attack on the substrate disulfide is mediated by the N-terminal thiolate anion of this motif. To evaluate the potential of TRP14 to act as a disulfide reductase and to compare such an ability with that of Trx1, we determined the pK_a values of TRP14 and Trx1. The pK_a of a Cys residue can be determined from the pH dependence of its reaction with alkylating reagents, which react preferentially with the ionized thiolate anion (5). From the pH dependence of the alkylation reaction with [^{14}C]iodoacetamide (Fig. 6*A*), the pK_a values for TRP14 and Trx1 were determined to be ~6.1 and ~7.3, respectively. The corresponding value for *E. coli* Trx is 6.7 (5). The N-terminal cysteine (Cys^{43}) of the C*XX*C motif appears to be responsible for this low pK_a value of TRP14, given that the C43S mutant was labeled poorly with iodoacetamide even at pH 8.0 (data not shown).

We also determined the standard-state redox potential ($E^{0'}$), another important determinant of reductase activity as previously described for *E. coli* Trx (34). The $E^{0'}$ value of TRP14, calculated on the basis of the equilibrium established between NADPH and recombinant TRP14 in the presence of TrxR1 at pH 7.0 and 25 °C, were −257 mV (Fig. 6*B*). This value is similar to those of other cellular reductants including *E. coli* Trx (−270 to −267 mV) (34, 35), three *E. coli* isoforms of Grx (−233 to −198 mV) (36), and GSH (−240 mV) (36). We attempted to measure the $E^{0'}$ value of Trx1 but failed. This is probably because, unlike *E. coli* Trx, mammalian Trx1 proteins contain three additional Cys residues in addition to the two in their active site and one of them, Cys^{73}, forms an intermolec-

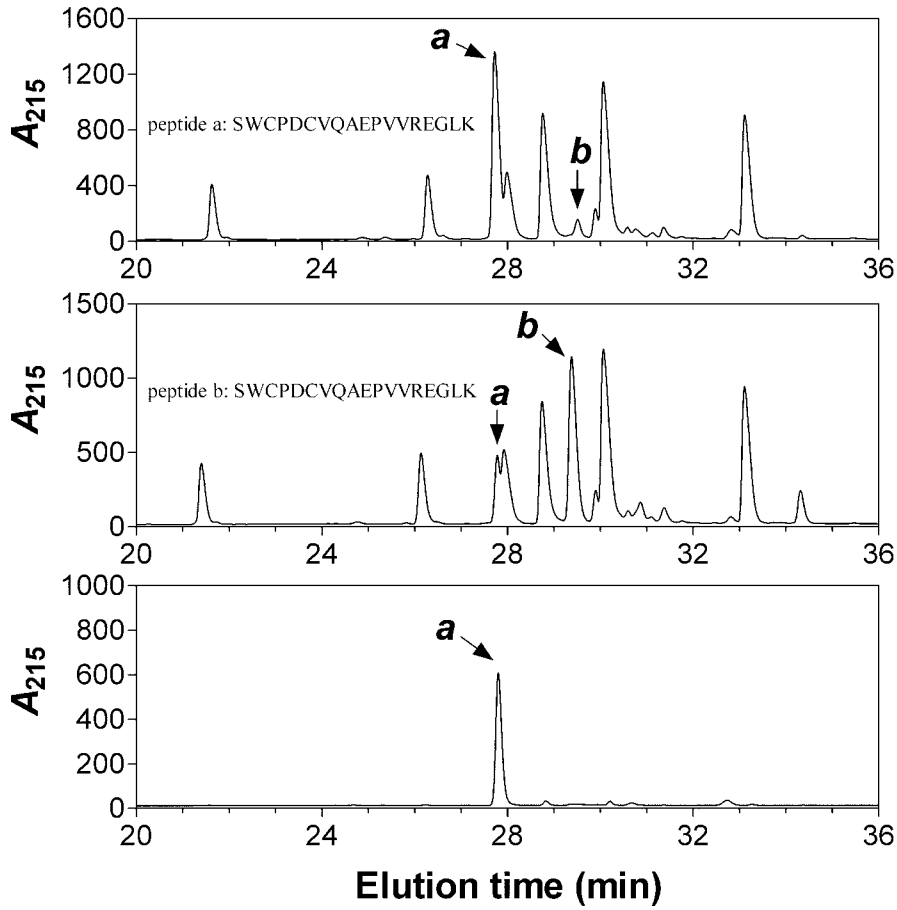

FIG. 3. **HPLC analysis of peptides generated by Lys-C from iodoacetamide-labeled TRP14.** Reduced (*top panel*) and oxidized (*middle panel*) forms of TRP14 were labeled with iodoacetamide by incubation for 30 min at room temperature in a reaction mixture containing 50 mM Tris-HCl (pH 8.5), 1 mM EDTA, 6 M guanidinium chloride, 5 mM iodoacetamide, and 20 μM protein. After isolation by ultrafiltration, the iodoacetamide-labeled protein (100 μg) was digested overnight at room temperature with Lys-C (5 μg) in 0.5 ml of 20 mM Tris-HCl (pH 8.0) containing 1 mM EDTA and 10% acetonitrile. The resulting peptides were separated on a C_{18} reversed-phase column by HPLC with a linear gradient of 0 to 60% acetonitrile applied over 60 min at a flow rate of 1 ml/min; elution was monitored at 215 nm. Oxidation of TRP14 was associated with a decrease in the size of peak *a* and an increase in that of peak *b*, and the peptides corresponding to these peaks were sequenced. Peptide *b* from the oxidized protein (*middle panel*) was reduced with 1 mM DTT, labeled with iodoacetamide, and analyzed by HPLC (*bottom panel*).

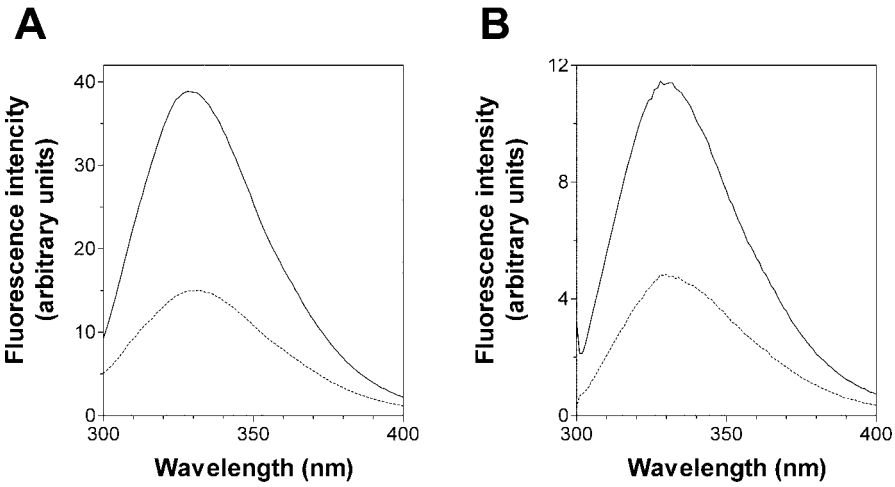

FIG. 4. **Fluorescence emission spectra of oxidized and reduced TRP14.** Protein fluorescence was measured with a thermostated spectrofluorimeter (Photon Technology International) at 25 °C. After excitation at 280 nm (*A*) or 295 nm (*B*), fluorescence emission spectrum from 300 to 400 nm of oxidized (*dotted*) or reduced (*solid*) TRP14 was recorded. The bandwidth of the excitation and emission were 5 nm. The samples contained 1 μM TRP14 in 0.2-ml of 100 mM sodium phosphate (pH 7.0) and 1 mM EDTA. Reduction of oxidized TRP14 was achieved by addition of dithiothreitol to the final concentration of 1 mM. Appropriate solvent blanks were run and subtracted from the sample spectra.

ular disulfide, which is relatively insensitive to reduction by TrxR1 (37).

Trx1 and TrxR1 couple the ribonucleotide reductase activity of RNR, the methionine sulfoxide reductase activity of MSR, and the peroxidase activity of Prx to NADPH oxidation by reducing the disulfide-containing enzyme intermediates (6–9). We compared the abilities of TRP14 and Trx1 to support these enzyme activities by monitoring NADPH oxidation in the presence of TrxR1 and NADPH (Fig. 7). The activity supported by TRP14 was only 2–4% of that supported by Trx1 for all three enzymes, suggesting that TRP14 is a poor electron donor for the oxidized forms of RNR, MSR and Prx.

We next measured the disulfide reductase activities of TRP14 and Trx1 toward insulin (5700 Da), which contains one intramolecular and two intermolecular disulfides. Disulfide reductase activity was monitored by detection of free SH groups with DTNB. Although TRP14 exhibited a concentration-dependent disulfide reductase activity toward insulin, this activity was much smaller than that of Trx1 (Fig. 8*A*). Reductase activity was also measured with oxytocin and vasopressin, both of which comprise nine amino acids and contain an intramolecular disulfide. The initial reaction rates with either peptide substrate were similar for TRP14 and Trx1, but the rate of each TRP14 reaction slowed markedly with time (Fig. 8, *B* and *C*). This slowing was probably attributable to the K_m values of TRP14 for the two peptides being higher than the concentration (0.1 mM) of the peptides used in the assay; the rates thus gradually decreased as the substrate was depleted (75–80% of each peptide was estimated to be reduced during 200 s on the basis of the decrease in A_{340}). The constant rate of the Trx1

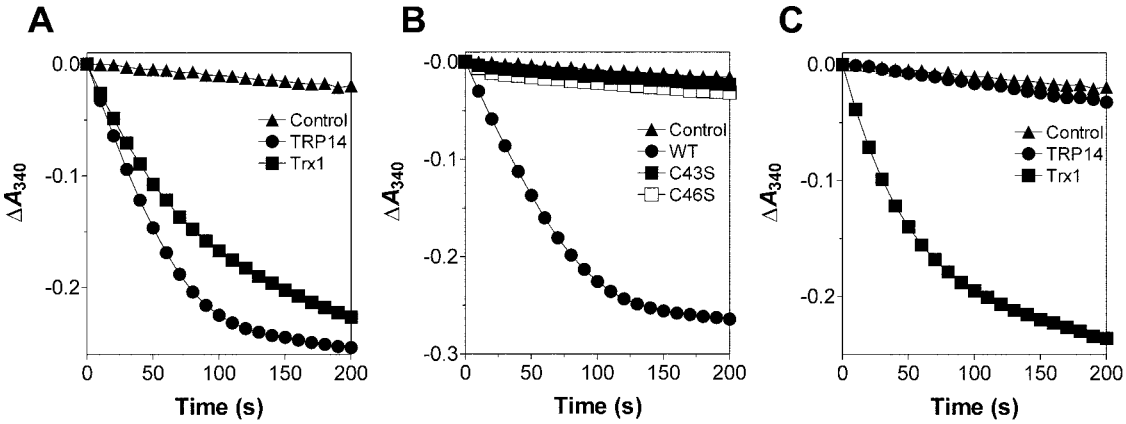

FIG. 5. **Reduction of TRP14 and Trx1 by TrxR1 or TrxR2.** *A*, reduction of oxidized TRP14 and Trx1 by TrxR1 was assayed at 30 °C by monitoring A_{340} in a 0.2-ml reaction mixture containing 50 mM HEPES-NaOH (pH 7.0), 1 mM EDTA, 0.2 mM NADPH, 50 nM TrxR1, and 50 μM oxidized TRP14 or Trx1. A reaction mixture lacking TrxR1 served as a control. *B*, reduction of wild-type (WT) TRP14 and of the cysteine mutants C43S and C46S by TrxR1 was performed as described in *A*. *C*, reduction of oxidized TRP14 and Trx1 by TrxR2 was assayed as in *A* with the exception that TrxR1 was replaced by TrxR2.

TABLE II

Kinetic parameters for the reduction of TRP14 and Trx1 by TrxR1

The reaction was initiated by the addition of various concentrations of oxidized TRP14 or Trx1 to an assay mixture containing 50 mM HEPES-NaOH (pH 7.0), 1 mM EDTA, 0.2 mM NADPH, and 25 nM TrxR1. The initial velocity was calculated by measuring the decrease in A_{340} at 30 °C.

	k_{cat}	K_m	k_{cat}/K_m
	min^{-1}	μM	$min^{-1}\ \mu M^{-1}$
TRP14	1297.2	8.3	156.3
Trx1	1233.2	10.8	114.2

reactions apparent until near completion of reduction indicates that the K_m values of Trx1 for the two peptides are substantially less than 0.1 mM.

Peroxidase Activity of TRP14—Trx1 alone has been suggested to act as an antioxidant that scavenges H_2O_2 (4). The reactive C*XX*C motif readily undergoes oxidation-reduction in the presence of H_2O_2, NADPH, and TrxR. TRP14 was also shown to be capable of reducing H_2O_2; its specific activity measured in the presence of 1 mM H_2O_2 was 23 nmol/min per milligram, which was about four times that of Trx1 (Fig. 9*A*). This peroxidase activity of TRP14 was attributable to the C*XX*C motif, given that the C43S mutant did not reduce H_2O_2 (Fig. 9*A*). The peroxidase activity of TRP14 was dependent on enzyme concentration (Fig. 9*B*) and H_2O_2 concentration (Fig. 9*C*). The H_2O_2 concentration dependence of the reaction yielded a K_m value of >3–5 mM, suggesting that TRP14 is not likely to contribute substantially to peroxidase activity in cells. Some peroxidases exhibit differential activity with lipid peroxides and H_2O_2 (38). Experiments with cumene peroxide and *t*-butyl peroxide revealed that the activity of TRP14 with H_2O_2 is markedly greater than that with hydrophobic peroxides (Fig. 9*D*).

DISCUSSION

Cellular redox status undergoes substantial changes in association with various cellular processes (39–42). For example, most proliferating cells maintain a more reducing environment (estimated redox potential of about −240 mV) compared with that of differentiated cells (about −200 mV) and even more so compared with that of apoptotic cells (about −170 mV) (39–41). Such changes in the intracellular redox environment are necessary for a cell to progress through the cell cycle or to undergo apoptosis (42, 43). The cellular redox potential is determined predominantly by the concentrations of reduced and oxidized coenzymes such as NAD(P)H-NAD(P) and GSH-GSSG (42). Changes in cellular redox potential result in an altered redox state of many protein sulfhydryl groups as a direct result of oxidation to disulfide by ROS or of reduction of the disulfide by disulfide reductases such as Trx. Given its negative redox potential of around −270 mV, reduced Trx might be expected to be capable of reducing almost all disulfide bonds in proteins; however, its action appears to be limited to specific target proteins with which it physically interacts. This requirement for specific interaction would be expected to restrict the number of substrates for a given Trx molecule and therefore necessitate the existence of a variety of Trx isoforms or Trx-related proteins (TRPs).

All organisms from bacteria to mammals contain multiple Trx isoforms. Although the amino acid sequences of Trx proteins from different species are not highly conserved, they all contain the conserved catalytic sequence C*XX*C. At least 35 Trx isoforms or TRPs containing this consensus sequence have been identified in *Arabidopsis thaliana*, and some of these Trx and TRP isoforms exhibited substrate specificity *in vitro* (44, 45). Multiple Trx isoforms and TRPs have also been identified in mammalian cells. The Trx2 isoform is a mitochondrial protein with the active site sequence WCGPC and shares 35% amino acid sequence identity with the cytosolic Trx1 (33). Another Trx isoform, designated Sptrx, is expressed specifically in spermatozoa and also contains the active site sequence WCGPC; its Trx domain shares 25% amino acid sequence identity with Trx1 but it also possesses a substantial N-terminal extension consisting of repeated motifs of unknown function (46). In addition, three mammalian TRPs have been identified previously: a 32-kDa cytosolic protein (TRP32) with the active site sequence WCGPC (47), a 32-kDa transmembrane protein (TMX) with the active site sequence WCPAC (48), and a 48-kDa nucleoredoxin (Nrx) with the active site sequence WCPPC (49). However, none of these Trx isoforms or TRPs has been well characterized in terms of biochemical properties or physiological functions.

The disulfide reductase activity of C*XX*C-containing proteins depends on various factors, one of the most important of which is the acidic character of the thiol group of the exposed cysteine, usually the N-terminal Cys of the motif. The pK_a of this residue is 1 to 2 units lower than that of the normal value of 8.5, with the result that it exists in the thiolate form at neutral pH. The exposed thiolate anion is required to initiate nucleophilic attack on the disulfide of the substrate protein. However, if the pK_a of this residue is too low, the dissociation of the transient mixed disulfide formed with the substrate becomes slow (36).

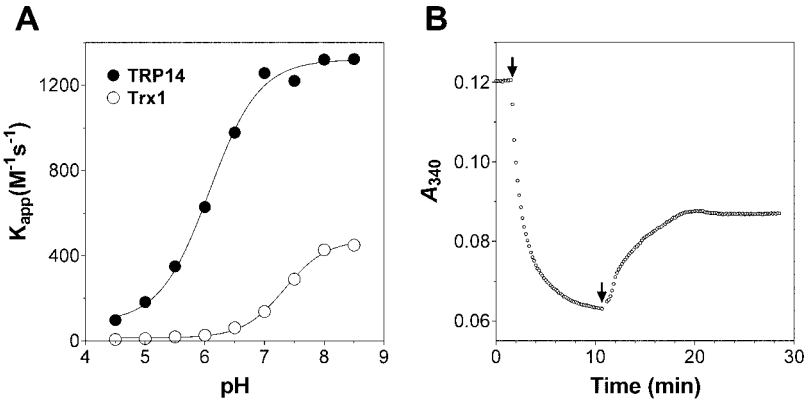

FIG. 6. **Determination of pK_a value (*A*) and redox potential (*B*) for human TRP14.** *A*, the reaction was initiated by the addition of 10 μM TRP14 or Trx1 to a mixture containing 10 μM iodo[1-^{14}C]acetamide (59.0 Ci/mol), 1 mM EDTA, and 100 mM buffer (sodium acetate (pH 4.5 and 5.0), MES-HCl (pH 5.5 to 6.5), HEPES-NaOH (pH 7.0 and 7.5), or Tris-HCl (pH 8.0 and 8.5)). After incubation for 1 min at room temperature, the reaction was stopped by the addition of 1% phosphoric acid and samples were spotted on P81 cellulose phosphate paper (Whatman). The paper was washed twice with 1% phosphoric acid, rinsed with acetone, and assayed for associated ^{14}C radioactivity. *B*, the reaction was initiated at 25 °C by the addition of 7.5 nM TrxR1 (*first arrow* in the time course) to a mixture containing 0.1 M sodium phosphate (pH 7.0), 1 mM EDTA, 20 μM NADPH, and 10 μM TRP14. After the reaction had reached equilibrium, 1 mM $NADP^+$ was added (*second arrow*) to generate a new equilibrium. The formation of NADPH was monitored from the increase in A_{340}. The extinction coefficients for NADPH (340 nm) and $NADP^+$ (260 nm) were 6.2 and 15.3 mM^{-1} cm^{-1}, respectively. The $E^{0'}$ values were calculated from the equation $3E^{0'} = 3E^{0'}NADP+ + (3RT/3nF)\ln([redTRP14][NADP^+]/[oxTRP14][NADPH])$ with a value of −0.315 for $E^{0'}{}_{NADP+}$.

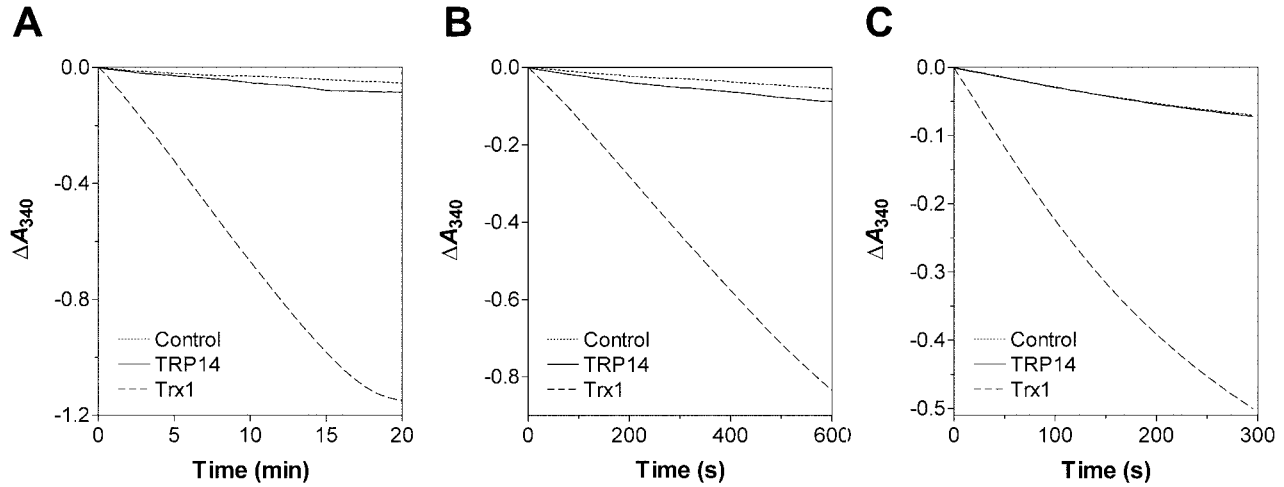

FIG. 7. **TRP14- or Trx-supported enzymatic activities of RNR (*A*), MSR (*B*), and Prx (*C*).** The reactions were performed at 30 °C in a final volume of 200 μl and were monitored on the basis of A_{340}. An assay mixture lacking TRP14 and Trx1 served as a control. The RNR reaction mixture contained 50 mM HEPES-KOH (7.6), 100 mM KCl, 6.4 mM $MgCl_2$, 3 mM ATP, 20 μM $FeCl_3$, 1.2 μM R1, 2.4 μM R2, 0.2 mM NADPH, 50 nM TrxR1, 5 μM TRP14 or Trx1, and 0.5 mM CDP. The MSR reaction mixture contained 50 mM Tris-HCl (pH 7.5), 1 mM EDTA, 0.2 mM NADPH, 50 nM TrxR1, MSR (5 μg/ml), 5 μM TRP14 or Trx1, and 3 mM methionine sulfoxide. The Prx reaction mixture contained 50 mM HEPES-NaOH (pH 7.0), 1 mM EDTA, 0.2 mM NADPH, 50 nM TrxR1, 2.5 μM PrxI, 5 μM TRP14 or Trx1, and 0.1 mM H_2O_2.

Another important determinant of disulfide reductase activity is whether the redox potential of the C*XX*C domain is sufficiently low to allow the supply of electrons to the substrate. Certain C*XX*C proteins, such as protein-disulfide isomerases, serve as electron acceptors and promote disulfide formation as a result of their high redox potentials ($E^{0'}$ = −180 mV) (50). Although low pK_a and low $E^{0'}$ values are required for disulfide reductase activity, they do not ensure such activity. The orientation of the oxidized substrate relative to the C*XX*C protein must thus be correct for the reductase reaction to occur. Reduction of the target cystine is also governed by specific interactions between the electron donor and acceptor molecules (25). For continuous enzyme action, the oxidized C*XX*C motif of the reductase must be reduced by TrxR. In this regard, TRP32 is not likely to function as a reductase because its oxidized form is not readily reduced by TrxR or even by dithiothreitol (4, 47).

We have now shown that TRP14 is a widely expressed (Fig. 2), 123-amino acid protein with a WCPDC motif, which differs from the consensus active site sequence of WCGPC for Trx isoforms (Fig. 1). The amino acid sequences of TRP14 and Trx1 are also less related (20% identity) than are those of mammalian Trx isoforms (25–35% identity). Although TRP14 contains five cysteines, only the two Cys residues in its WCPDC motif are exposed and susceptible to oxidation by H_2O_2 to a disulfide (Table I and Fig. 3). And oxidation of these two cysteine residues caused to decrease fluorescence intensity due to Trp^{77} and Trp^{42} (Fig. 4). The oxidized form of TRP14 was readily reduced by TrxR1 with kinetic parameters that were slightly more favorable than those for Trx1 reduction (Fig. 5*A* and Table II). Oxidized TRP14 was not a substrate for the mitochondrial TrxR2, however (Fig. 5*C*). TRP14 is thus distinguishable from Trx1 and Trx2, both of which are efficiently reduced by both the cytosolic and mitochondrial TrxR enzymes.

The redox potential ($E^{0'}$ = −257 mV) of TRP14 (Fig. 6*B*) is similar to those of other thiol reductants such as *E. coli* Trxs (−270 to −267 mV), *E. coli* Grxs (−233 to −198 mV), and GSH (−240 mV) (34–36). The pK_a of the N-terminal Cys of the TRP14 C*XX*C motif was determined to be 6.1 (Fig. 6*A*), which

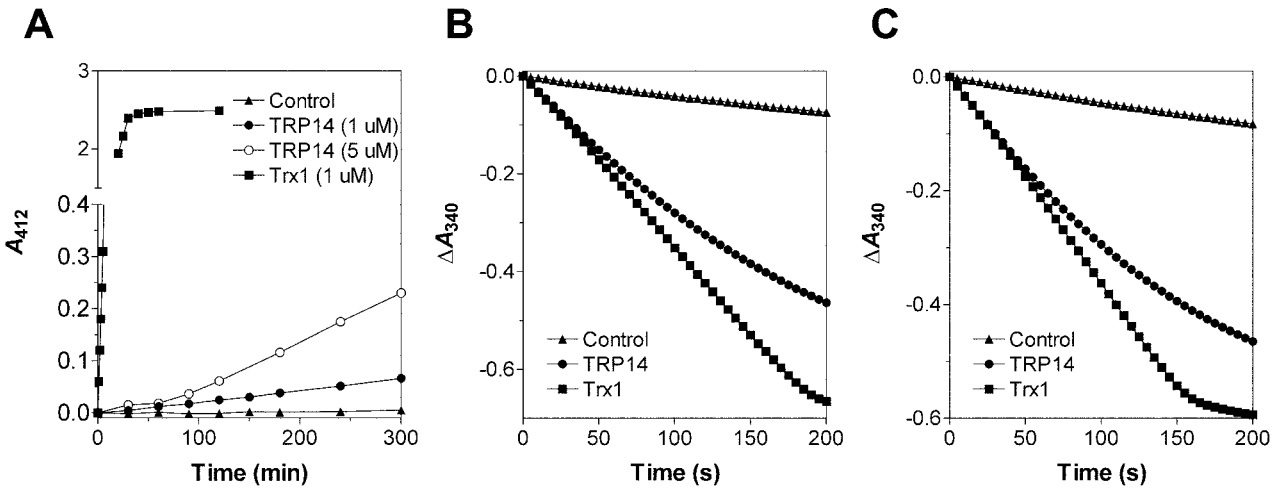

FIG. 8. **Reduction of insulin (*A*), oxytocin (*B*), and vasopressin (*C*) by TRP14 or Trx1.** The reduction reactions were performed at 30 °C, and assay mixtures lacking TRP14 and Trx1 served as controls. *A*, the incubation mixture contained 100 mM HEPES-NaOH (pH 7.6), 1 mM EDTA, 0.8 mM NADPH, 25 nM TrxR1, and either 1 or 5 μM TRP14 or 1 μM Trx1 in a final volume of 200 μl. The reaction was initiated by the addition of insulin to a final concentration of 340 μM. At the indicated times, 20 μl of the reaction mixture were removed and mixed with 180 μl of a solution containing 6 M guanidinium chloride, 100 mM sodium phosphate (pH 7.3), 1 mM EDTA, and 0.1 mM DTNB. The appearance of free SH groups was monitored on the basis of A_{412}. *B* and *C*, the assay was started by the addition of oxytocin or vasopressin, respectively, at a final concentration of 100 μM to a reaction mixture containing 50 mM HEPES-NaOH (pH 7.0), 1 mM EDTA, 0.2 mM NADPH, 50 nM TrxR1, and 5 μM TRP14 or Trx1. Peptide reduction was monitored on the basis of A_{340}.

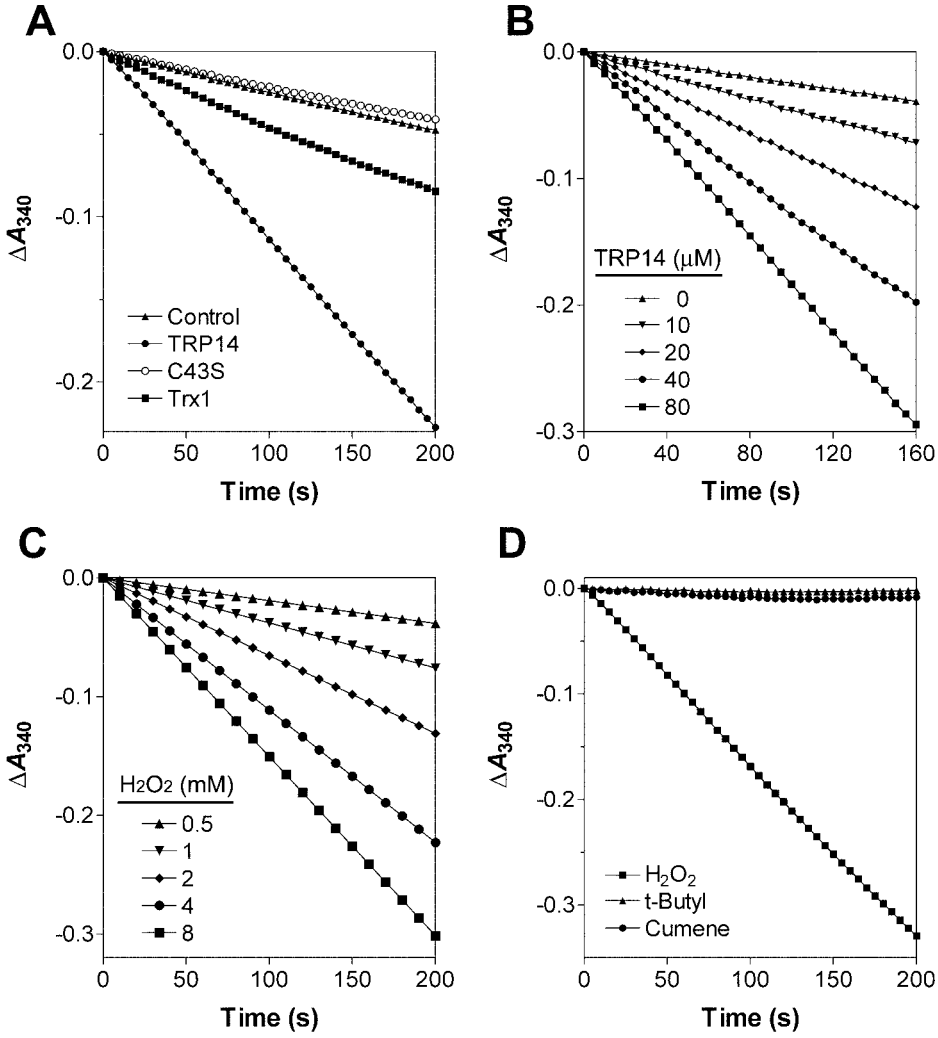

FIG. 9. **Peroxidase activities of TRP14 and Trx1.** Peroxidase reactions were performed at 30 °C and monitored on the basis of A_{340}. Assay mixtures lacking TRP14 and Trx1 served as controls. *A*, peroxidase activities of TRP14, the TRP14 mutant C43S, and Trx1 toward H_2O_2. The reaction mixtures contained 50 mM HEPES-NaOH (pH 7.0), 1 mM EDTA, 0.2 mM NADPH, 50 nM TrxR1, 1 mM H_2O_2, and 30 μM TRP14 or Trx1. *B*, TRP14 concentration dependence of the reduction of 1 mM H_2O_2. *C*, H_2O_2 concentration dependence of the peroxidase activity of 10 μM TRP14. *D*, reduction of H_2O_2, cumene peroxide, and *t*-butyl peroxide by TRP14. The reduction assay was performed as in *A* with 10 μM TRP14 and 10 mM peroxide.

would be predicted to result in a nucleophilicity greater than that of the corresponding Cys of Trx1 (pK_a = 7.3). However, TRP14 exhibited negligible disulfide reductase activity toward RNR, Prx, and MSR (Fig. 7), all of which are physiological substrates of Trx1, and it manifested a markedly lower activity than Trx1 toward the nonphysiological substrate insulin (Fig. 8*A*). In contrast, the small disulfide-containing peptides oxytocin and vasopressin were each reduced by TRP14 and Trx1 at

similar rates at saturating substrate concentrations (Fig. 8, *B* and *C*). In addition, as shown in the accompanying article (52), reduced TRP14 neither bound to nor inhibited the activity of ASK1, which is a component of TNF-α signaling cascades and associates strongly with reduced Trx1. Oxidized TRP14 and Trx1 also exhibit different specificities for TrxR enzymes. These data suggest that TRP14 might be highly selective in terms of its substrate and interacting proteins, possibly as a result of strict requirements for protein-protein interaction. Indeed the x-ray crystal structure of TRP14 [2] indicates that several negatively charged residues protruding from the binding surface may significantly restrict the number of substrates that can interact with TRP14. The x-ray structure also indicates that the high selectivity of TRP14 is not likely due to restricted access to its active site. The potential substrate binding surface of TRP14 is flat as that of Trx1, and the Cys^{43} of TRP14 is accessible as the Cys^{32} of Trx1 for disulfide bond formation with other proteins.

Trx proteins have also been suggested to remove peroxides directly. TRP14 was able to remove H_2O_2 in the presence of TrxR1 and NADPH but with a low catalytic efficiency (Fig. 9), suggesting that it does not function as a peroxidase for H_2O_2 or lipid peroxides in cells. In addition, unlike Trx, which contributes indirectly to the removal of peroxides by supporting the catalytic activity of Prx enzymes, TRP14 did not support the activity of Prx. It is therefore unlikely that the physiological roles of TRP14 include peroxide removal.

Many TNF-α-induced signaling pathways are redox sensitive and modulated by Trx1. In the accompanying article (52), the possible role of TRP14 in TNF-α signaling was studied in comparison with Trx1 through RNA interference, and LC8 dynein light chain was identified as a potential target protein of TRP14. Although the amount of TRP14 is only one-sixth that of Trx1 in HeLa cells, the effects of partial depletion of TRP14 on most of the TNF-α-induced signaling pathways were more pronounced than those of Trx1 depletion, suggesting that TRP14 and Trx1 likely act on different target proteins in TNF-α signaling pathways.

Acknowledgments—We thank B. Cooperman for RNR and J. Moskovitz for MSR.

REFERENCES

1. Holmgren, A. (1985) *Annu. Rev. Biochem.* **54,** 237–271
2. Nakamura, H., Nakamura, K., and Yodoi, J. (1997) *Annu. Rev. Immunol.* **15,** 351–369
3. Holmgren, A. (2000) *Antioxid. Redox. Signal* **2,** 811–820
4. Hirota, K., Nakamura, H., Masutani, H., and Yodoi, J. (2002) *Ann. N. Y. Acad. Sci.* **957,** 189–199
5. Kallis, G. B., and Holmgren, A. (1980) *J. Biol. Chem.* **255,** 10261–10265
6. Stubbe, J., and Riggs-Gelasco, P. (1998) *Trends Biochem. Sci.* **23,** 438–443
7. Chae, H. Z., Chung, S. J., and Rhee, S. G. (1994) *J. Biol. Chem.* **269,** 27670–27678
8. Kang, S. W., Baines, I. C., and Rhee, S. G. (1998) *J. Biol. Chem.* **273,** 6303–6311
9. Stadtman, E. R., Moskovitz, J., Berlett, B. S., and Levine, R. L. (2002) *Mol. Cell Biochem.* **234–235**, 3–9
10. Lee, S.-R., Yang, K.-S., Kwon, J., Lee, C., Jeong, W., and Rhee, S. G. (2002) *J. Biol. Chem.* **277,** 20336–20342

[2] J. R. Woo and S. E. Ryu, unpublished results.

11. Hirota, K., Murata, M., Sachi, Y., Nakamura, H., Takeuchi, J., Mori, K., and Yodoi, J. (1999) *J. Biol. Chem.* **274,** 27891–27897
12. Takeuchi, J., Hirota, K., Itoh, T., Shinkura, R., Kitada, K., Yodoi, J., Namba, T., and Fukuda, K. (2000) *Antioxid. Redox. Signal* **2,** 83–92
13. Meyer, M., Schreck, R., and Baeuerle, P. A. (1993) *EMBO J.* **12,** 2005–2015
14. Hirota, K., Matsui, M., Iwata, S., Nishiyama, A., Mori, K., and Yodoi, J. (1997) *Proc. Natl. Acad. Sci. U. S. A.* **94,** 3633–3638
15. Saitoh, M., Nishitoh, H., Fujii, M., Takeda, K., Tobiume, K., Sawada, Y., Kawabata, M., Miyazono, K., and Ichijo, H. (1998) *EMBO J.* **17,** 2596–2606
16. Gotoh, Y., and Cooper, J. A. (1998) *J. Biol. Chem.* **273,** 17477–17482
17. Liu, H., Nishitoh, H., Ichijo, H., and Kyriakis, J. M. (2000) *Mol. Cell. Biol.* **20,** 2198–2208
18. Nishiyama, A., Matsui, M., Iwata, S., Hirota, K., Masutani, H., Nakamura, H., Takagi, Y., Sono, H., Gon, Y., and Yodoi, J. (1999) *J. Biol. Chem.* **274,** 21645–21650
19. Joelson, T., Sjoberg, B. M., and Eklund, H. (1990) *J. Biol. Chem.* **265,** 3183–3188
20. Gleason, F. K., Lim, C. J., Gerami-Nejad, M., and Fuchs, J. A. (1990) *Biochemistry* **29,** 3701–3709
21. Chae, H. Z., Kim, H. J., Kang, S. W., and Rhee, S. G. (1999) *Diabetes Res. Clin. Pract* **45,** 101–112
22. Song, J. J., Rhee, J. G., Suntharalingam, M., Walsh, S. A., Spitz, D. R., and Lee, Y. J. (2002) *J. Biol. Chem.* **277,** 46566–46575
23. Kang, S. W., Chae, H. Z., Seo, M. S., Kim, K., Baines, I. C., and Rhee, S. G. (1998) *J. Biol. Chem.* **273,** 6297–6302
24. Rhee, S. G., Kang, S. W., Chang, T. S., Jeong, W., and Kim, K. (2001) *IUBMB Life* **52,** 35–41
25. Qin, J., Yang, Y., Velyvis, A., and Gronenborn, A. (2000) *Antioxid. Redox Signal* **2,** 827–840
26. Kim, J. R., Yoon, H. W., Kwon, K. S., Lee, S. R., and Rhee, S. G. (2000) *Anal. Biochem.* **283,** 214–221
27. Lee, S. R., Kim, J. R., Kwon, K. S., Yoon, H. W., Levine, R. L., Ginsburg, A., and Rhee, S. G. (1999) *J. Biol. Chem.* **274,** 4722–4734
28. Holmgren, A. (1972) *J. Biol. Chem.* **247,** 1992–1998
29. Krause, G., and Holmgren, A. (1991) *J. Biol. Chem.* **266,** 4056–4066
30. Slaby, I., Cerna, V., Jeng, M. F., Dyson, H. J., and Holmgren, A. (1996) *J. Biol. Chem.* **271,** 3091–3096
31. Arner, E. S., and Holmgren, A. (2000) *Eur. J. Biochem.* **267,** 6102–6109
32. Lee, S. R., Bar-Noy, S., Kwon, J., Levine, R. L., Stadtman, T. C., and Rhee, S. G. (2000) *Proc. Natl. Acad. Sci. U. S. A.* **97,** 2521–2526
33. Spyrou, G., Enmark, E., Miranda-Vizuete, A., and Gustafsson, J. (1997) *J. Biol. Chem.* **272,** 2936–2941
34. Lin, T. Y. (1999) *Biochemistry* **38,** 15508–15513
35. Mossner, E., Huber-Wunderlich, M., Rietsch, A., Beckwith, J., Glockshuber, R., and Aslund, F. (1999) *J. Biol. Chem.* **274,** 25254–25259
36. Aslund, F., Berndt, K. D., and Holmgren, A. (1997) *J. Biol. Chem.* **272,** 30780–30786
37. Weichsel, A., Gasdaska, J. R., Powis, G., and Montfort, W. R. (1996) *Structure* **4,** 735–751
38. Jeong, J. S., Kwon, S. J., Kang, S. W., Rhee, S. G., and Kim, K. (1999) *Biochemistry* **38,** 776–783
39. Cai, J., and Jones, D. P. (1998) *J. Biol. Chem.* **273,** 11401–11404
40. Kirlin, W. G., Cai, J., Thompson, S. A., Diaz, D., Kavanagh, T. J., and Jones, D. P. (1999) *Free Radic Biol. Med.* **27,** 1208–1218
41. Hutter, D. E., Till, B. G., and Greene, J. J. (1997) *Exp. Cell Res.* **232,** 435–438
42. Schafer, F. Q., and Buettner, G. R. (2001) *Free Radic Biol. Med.* **30,** 1191–1212
43. Li, N., and Oberley, T. D. (1998) *J. Cell. Physiol.* **177,** 148–160
44. Rouhier, N., Gelhaye, E., and Jacquot, J. P. (2002) *Ann. N. Y. Acad. Sci.* **973,** 520–528
45. Collin, V., Issakidis-Bourguet, E., Marchand, C., Hirasawa, M., Lancelin, J. M., Knaff, D. B., and Miginiac-Maslow, M. (2003) *J. Biol. Chem.* **278,** 23747–23752
46. Miranda-Vizuete, A., Ljung, J., Damdimopoulos, A. E., Gustafsson, J. A., Oko, R., Pelto-Huikko, M., and Spyrou, G. (2001) *J. Biol. Chem.* **276,** 31567–31574
47. Lee, K. K., Murakawa, M., Takahashi, S., Tsubuki, S., Kawashima, S., Sakamaki, K., and Yonehara, S. (1998) *J. Biol. Chem.* **273,** 19160–19166
48. Matsuo, Y., Akiyama, N., Nakamura, H., Yodoi, J., Noda, M., and Kizaka-Kondoh, S. (2001) *J. Biol. Chem.* **276,** 10032–10038
49. Kurooka, H., Kato, K., Minoguchi, S., Takahashi, Y., Ikeda, J., Habu, S., Osawa, N., Buchberg, A. M., Moriwaki, K., Shisa, H., and Honjo, T. (1997) *Genomics* **39,** 331–339
50. Lundstrom, J., and Holmgren, A. (1993) *Biochemistry* **32,** 6649–6655
51. Riddles, P. W., Blakeley, R. L., and Zerner, B. (1983) *Methods Enzymol.* **91,** 49–60
52. Jeong, W., Chang, T.-S., Boja, E. S., Fales, H. M., and Rhee, S. G. (2004) *J. Biol. Chem.* **279,** 3151–3159

Identification and Characterization of TRP14, a Thioredoxin-related Protein of 14 kDa: NEW INSIGHTS INTO THE SPECIFICITY OF THIOREDOXIN FUNCTION

Woojin Jeong, Hae Won Yoon, Seung-Rock Lee and Sue Goo Rhee

J. Biol. Chem. 2004, 279:3142-3150.
doi: 10.1074/jbc.M307932200 originally published online November 7, 2003
